Neutron tomography using an elliptic focusing guide

N. Kardjilov,[1,a)] A. Hilger,[1] M. Dawson,[2] I. Manke,[3] J. Banhart,[3] M. Strobl,[4] and P. Böni[5]

[1]*Helmholtz Zentrum Berlin, Hahn-Meitner-Platz 1, 14109 Berlin, Germany*
[2]*Helmholtz Zentrum Berlin, Hahn-Meitner-Platz 1, 14109 Berlin, Germany and School of Computing,*
Science & Engineering, University of Salford, Salford, Greater Manchester M5 4WT, United Kingdom
[3]*Helmholtz Zentrum Berlin, Hahn-Meitner-Platz 1, 14109 Berlin, Germany and Berlin Institute of Technology,*
Straße des 17 Juni 135, 10623 Berlin, Germany
[4]*Ruprecht Karls University of Heidelberg, Im Neuenheimer Feld 253, 69120 Heidelberg, Germany and*
Helmholtz Zentrum Berlin, Hahn-Meitner-Platz 1, 14109 Berlin, Germany
[5]*Fakultät für Physik, Technische Universität München, E21, 85748 Garching, Germany*

An elliptic focusing neutron guide was combined with a cold neutron imaging instrument to produce a cone-beam, whose parameters were then characterized both at the focal point and at the detector position. This point source geometry provides improved experimental conditions for tomographic applications, providing a larger beam cross-section and enabling geometric magnification. The experimental data were compared with Monte Carlo simulations and both experiments and simulations demonstrate superior spectral and geometric homogeneity of the cone-beam setup compared to the conventional pinhole geometry. © *2010 American Institute of Physics*. [doi:10.1063/1.3467796]

I. INTRODUCTION

Neutron tomography (NT) has gained significant importance as a nondestructive method for the investigation of the composition of bulk materials in various fields of science and technology[1,2] and new experimental methods such as phase-contrast, energy-selective, dark-field, and polarized neutron imaging have witnessed substantial development.[3–13] In addition, innovative detector systems overcome some of the limitations of conventional NT regarding spatial and temporal resolution.[14,15]

Most neutron imaging instruments are currently based on the simple pinhole geometry,[16] in which the best achievable spatial resolution is limited by the L/D ratio, where L is the distance between the "source" pinhole with a diameter D and the detector position.[17] The beam size at the detector position is defined by the beam divergence and the distance L. In order to achieve higher spatial resolution, it is necessary to keep L/D high (i.e., by increasing L/decreasing D) and to position the sample as close as possible to the detector such that the image of the sample projected onto the detector can be considered to be formed by a parallel-beam that is perpendicular to the detection plane.

If a neutron guide is positioned upstream of the pinhole, the beam divergence is determined by the angle of total reflection of the neutrons from the interior walls of the neutron guide.[16,17] This angle depends on the neutron wavelength and causes a spectral heterogeneity of the beam downstream of the guide. The divergence (and therefore available beam size) at the detector position is thus also determined by the coating of the neutron guide.

Here we demonstrate how neutron radiography and tomography can benefit from a focusing neutron guide producing a well-defined cone-beam.[18] According to Liouville's

theorem, the phase space volume occupied by the neutron beam is invariant and the spatial compression of the beam into a focal point thus implies an increased beam divergence.[19–22] The geometry used is similar to the configuration applied in microfocus x-ray computed tomography scanners, where the x-rays emerge from a spot of a few micrometers diameter. The cone-beam geometry allows a variable magnification by altering the position of the sample with respect to the source and the detector.

II. SIMULATIONS

Two focusing neutron guides (linear taper and elliptic) and a straight neutron guide with circular pinhole (for comparison) each of total length 3 m were simulated using the Monte Carlo simulation code MCSTAS.[23] During the course of the simulation, cold neutrons were supplied by a curved neutron guide (cross section: 30×120 mm^2, length: 20 m, radius of curvature 3000 m) with a coating of ^{58}Ni, which gives 1.2 times the critical angle θ_c of natural Ni (m=1.2). A flight path of 5 m between the end of the secondary guide (straight, linear taper, and elliptic) and the detector plane represents the length of the real instrument, Fig. 1(a).

The intensity distribution measured at the detector position [Fig. 1(a)] shows that the elliptic guide provides an almost homogeneously illuminated area of approximately 20×20 cm^2. The observed segments in the image are due to the defined neutron spectral distribution [shown in Fig. 1(c)], which limits the range of the available total reflection angles and produces discontinuities in the image. The intensity gaps between the segments (seen as dark lines with approximately 15% intensity decrease) can be corrected by image normalization, which is a common procedure in digital radiography. The linearly tapered guide illuminates a similar area as the elliptic guide but with a less uniform radial intensity distri-

a)Electronic mail: kardjilov@helmholtz-berlin.de.

a)

b)
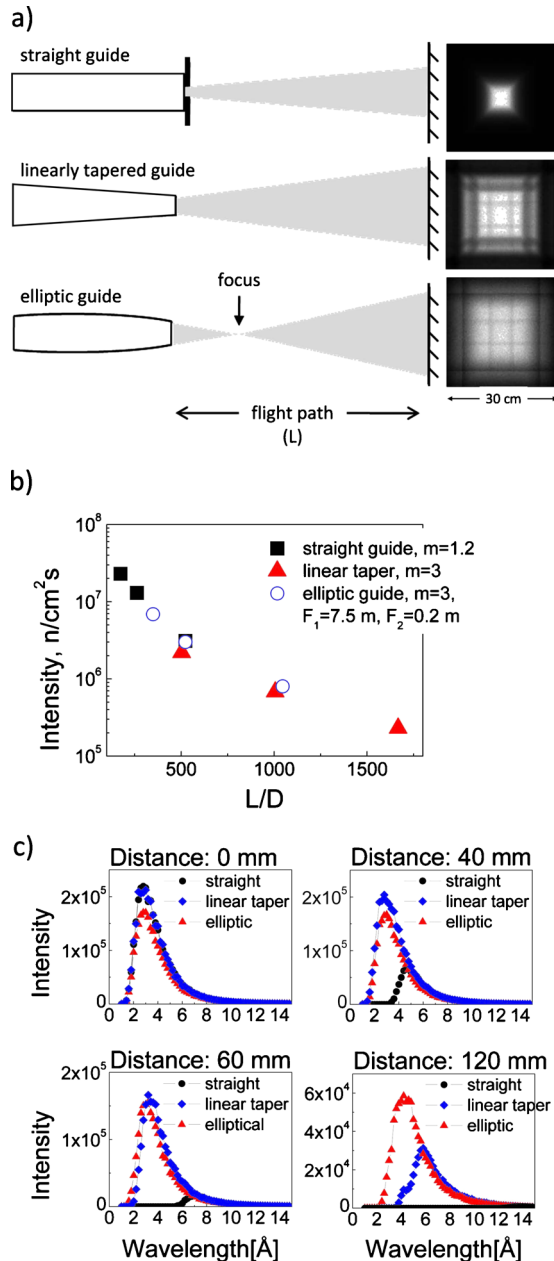
FIG. 1. (Color online) Monte Carlo simulations of different neutron guide configurations. (a) Intensity distribution 5 m behind the guide exit in a detector plane of 30×30 cm^2 for a straight guide with a pinhole of 1 cm; linearly tapered guide (coating m=3.0, length: 3 m, entrance: 3×3 cm^2, exit: 1×1 cm^2); elliptic guide (coating m=3.0, length: 3 m, entrance: 3×3 cm^2, exit: 0.89×0.89 cm^2, F_1=7.5 m, F_2=0.2 m). (b) Neutron flux integrated over the central area of the detector (1×1 cm^2) as a function of L/D. (c) Spectra calculated at different distances from the beam axis integrated over an area of 1×1 cm^2.

bution. The standard (straight guide with circular pinhole) configuration provides a beam that is just 1/9 the area of the beams produced by the focusing guides.

The simulated intensities at the detector position for a defined L/D ratio are depicted in Fig. 1(b). In order to simulate different L/D ratios, circular pinholes with various diameters D were placed at the exit of the guide system for the straight and linear taper setups and at the focal point of the elliptic guide. The distance between the exit of the guide and the detector plane was kept constant at L=5 m.
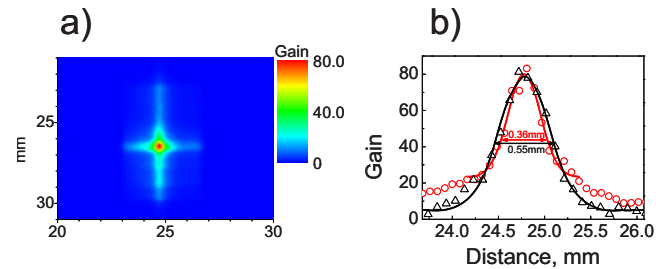
FIG. 2. (Color online) Characterization of the beam at the focal point of the elliptic guide. (a) Intensity distribution. (b) Horizontal ($\bigcirc$) and vertical ($\triangle$) intensity profiles were fitted by Gaussian functions.

The comparison shows that the neutron flux in the central part of the beam depends only on the L/D ratio but not on the neutron guide configuration [Fig. 1(b)]. A study of the spectral homogeneity shows (i) that for the elliptic setup the spectrum is essentially uniform, (ii) that transmitted by the linear tapered guide is almost uniform, except far away from the beam axis, while (iii) for the straight guide the spectrum softens rapidly toward the edges [Fig. 1(c)]. The reason for the superior behavior of the elliptic guide is that neutrons with the same wavelength (i.e., having the same angle of incidence) can have vastly different trajectories upon leaving the guide depending on the position at which total reflection took place; this helps to homogenize the spectral distribution at behind the focal point. The enlarged beam cross-section and improved spectral and intensity homogeneity of the elliptic guide are expected to lead to an improved performance in real applications.

III. EXPERIMENT

An elliptic guide was tested experimentally and results were compared with those obtained using a straight guide. The setup used a focusing elliptic neutron guide with a length of 500 mm, a rectangular cross sections of 10.6 $\times$ 21.2 mm^2 (entrance) and 4×8 mm^2 (exit) and a super-mirror coating m=3. The focal points were at a distance of F_1=1580 mm and F_2=80 mm from the exit of the guide. Note that these values are different from those used for the simulations in Fig. 1(b). Experiments were performed at Cold Neutron RADiography, the neutron imaging beamline at the Hahn-Meitner-Reactor of the Helmholtz-Zentrum Berlin.[24] The beam was characterized at F_2 using a cold neutron spectrum (maximum at 3 Å). To allow a comparison with the conventional geometry, gain factor images with and without the focusing guide were recorded.

Using the elliptic guide the width of the focal point in the central area of the beam was found to be 0.36 mm in the horizontal and 0.55 mm in the vertical direction (Fig. 2). The spot size was determined using Gaussian fits of the horizontal and vertical intensity profiles through the focal point. That the obtained full width at half maximum (FWHM) differ can be explained by the nonsymmetrical shape of the guide: The guide is larger in the vertical dimension. This means that in the central area there is a superposition of vertical and horizontal Gauss functions with different FWHM, while in the wings the neutrons come only from one focusing direction, either vertical or horizontal. The Gaussian parameters, there-

a)

b)

distance:

0.5 cm   60 cm   120 cm
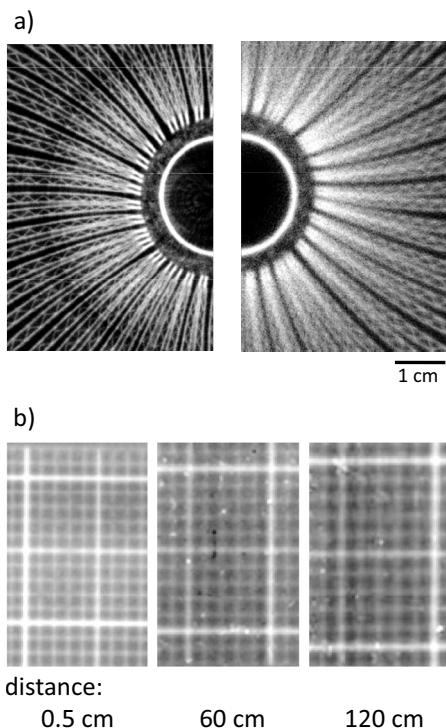
FIG. 3. Imaging experiments. (a) Tomographic slice of the central part of a particle filter measured in the cone-beam geometry (left) and parallel-beam scanning geometry (right). (b) Magnification of a grid with 1 mm periodicity measured at different distances from the detector (0.5 cm, 60 cm and 120 cm) in the cone-beam geometry.

fore, differ between the central area of the focal point and the wings. The focused white neutron beam shows a maximal intensity gain of 80 at the focal point (compared to the straight guide). The small size of the focal point is a good precondition for the realization of a point source geometry with a high L/D ratio. By changing the distance from the focal point, the desired beam size can be selected, and by placing a suitable pinhole with a diameter D at the focal point the L/D ratio can be adjusted.

IV. APPLICATIONS

The cone-beam geometry enables large beam cross sections at relative short distances from the focal point. Use of the elliptic guide discussed above allowed enlargement of the beam dimensions by a factor of 3 at a distance of 5 m from the end of the guide to the detector at CONRAD, thus enabling tomographic investigations of large samples. Additionally, the small focal point provides a good L/D ratio, which is important for achieving high spatial resolution—particularly concerning experiments involving samples that cannot be placed close to the detector plane.

This configuration has been used to investigate a particle filter for a diesel engine (15 cm diameter) at a distance of 4.2 m between the focal point (80 mm from the guide exit) and the detector plane. 600 projections of the sample were recorded at equidistant angular steps with a total rotation of 360°, and the data were reconstructed using an algorithm for cone-beam geometry [Fig. 3(a) left]. A measurement using a straight guide and a circular pinhole with $D=2$ cm and identical data collection parameters was also performed; the data

were reconstructed using a filtered back-projection algorithm assuming parallel-beam geometry [Fig. 3(a) right]. In this case the sample had to be scanned through the beam in order to illuminate it completely since the sample was larger than the beam cross-section. The width of the pinhole was chosen such that the initial flux was identical to the elliptic setup by providing a similar area (3.14 cm^2) to the entrance area of the elliptical guide (2.25 cm^2). The ratio of the entrance areas of the pinhole to the guide: $3.14/2.25=1.39$ correlates well with the ratio of exposure times per projection: 60 s/45 s$=1.33$. The comparison, Fig. 3 shows that the quality of the reconstruction is markedly improved using the cone-beam setup.

However, the cone-beam reconstruction includes radial artifacts owing to beam inhomogeneities caused by the joints of the segments of the supplying neutron guide upstream of the focusing guide. These discontinuities become visible in the projection images due to the "camera-obscura" geometry. The scanning of the sample across the beam required in the straight guide geometry effectively smeared out these artifacts across the image making them less noticeable.

The possibility for magnification provided by the cone-beam setup was studied by visualizing a periodic grid (Gd mask deposited on Si wafer) with a periodicity of 1 mm. The measurement at 1.2 m distance from the detector shows a magnification of 20% [right hand side of Fig. 3(b)].

V. CONCLUSION

We have shown that the installation of an elliptic guide allows the realization of a beamline for NT using a cone-beam geometry. The advantages are a larger beam cross-section at the sample position and an improved spatial and spectral homogeneity of the beam. In addition, by decreasing the size of the pinhole at the focal position of the elliptic guide, the L/D ratio can be increased thus achieving higher resolution. The magnification of the sample by the cone-beam allows the option using highly efficient detectors that would otherwise give only limited spatial resolution. It is forseen that by increasing the critical angles of the supermirror coatings to above m=7 (Ref. 25) and by using modified guide geometries, the beam size in the focal position can be decreased to below 20 μm, thus providing very high spatial resolution.

[1]J. Banhart, *Advanced Tomographic Methods in Materials Research and Engineering* (Oxford University Press, New York, 2008).
[2]N. Kardjilov, A. Hilger, I. Manke, M. Strobl, M. Dawson, and J. Banhart, Nucl. Instrum. Methods Phys. Res. A **605**, 13 (2009).
[3]F. Pfeiffer, C. Grünzweig, O. Bunk, G. Frei, E. Lehmann, and C. David, Phys. Rev. Lett. **96**, 215505 (2006).
[4]N. Kardjilov, A. Hilger, I. Manke, M. Strobl, W. Treimer, and J. Banhart, Nucl. Instrum. Methods Phys. Res. A **542**, 16 (2005).
[5]N. Kardjilov, I. Manke, M. Strobl, A. Hilger, W. Treimer, M. Meissner, T. Krist, and J. Banhart, Nat. Phys. **4**, 399 (2008).
[6]M. Dawson, N. Kardjilov, I. Manke, M. Strobl, A. Hilger, and J. Banhart,

British Institute of Radiology, Highlight Newsletter, Autumn 2008.

[7]C. Grünzweig, C. David, O. Bunk, M. Dierolf, G. Frei, G. Kühne, R. Schäfer, S. Pofahl, H. M. R. Rønnow, and F. Pfeiffer, Appl. Phys. Lett. **93**, 112504 (2008).

[8]N. Kardjilov, S. Baechler, M. Bastürk, M. Dierick, J. Jolie, E. Lehmann, T. Materna, B. Schillinger, and P. Vontobel, Nucl. Instrum. Methods Phys. Res. A **501**, 536 (2003).

[9]E. Lehmann, K. Lorenz, E. Steichele, and P. Vontobel, Nucl. Instrum. Methods Phys. Res. A **542**, 95 (2005).

[10]M. Strobl, C. Grünzweig, A. Hilger, I. Manke, N. Kardjilov, C. David, and F. Pfeiffer, Phys. Rev. Lett. **101**, 123902 (2008).

[11]M. Strobl, A. Hilger, N. Kardjilov, S. Keil, O. Ebrahimi, and I. Manke, Nucl. Instrum. Methods Phys. Res. A **605**, 9 (2009).

[12]M. Strobl, W. Treimer, P. Walter, S. Keil, and I. Manke, Appl. Phys. Lett. **91**, 254104 (2007).

[13]W. Treimer, M. Strobl, N. Kardjilov, A. Hilger, and I. Manke, Appl. Phys. Lett. **89**, 203504 (2006).

[14]G. Frei, E. H. Lehmann, D. Mannes, and P. Boillat, Nucl. Instrum. Methods Phys. Res. A **605**, 111 (2009).

[15]A. S. Tremsin, J. B. McPhate, J. V. Vallerga, O. H. W. Siegmund, J. S. Hull, W. B. Feller and E. Lehmann, Nucl. Instrum. Methods Phys. Res. A **604**, 140 (2009).

[16]B. Schillinger, M. Bleuel, P. Böni, and E. Steichele, *Seventh World Conference on Neutron Radiography*, edited by P. Chirco and R. Rosa (ENEA, Rome, Italy, 2005), p. 11.

[17]B. Schillinger, Nondestr. Test. Eval. **16**, 141 (2001).

[18]P. Böni, Nucl. Instrum. Methods Phys. Res. A **586**, 1 (2008).

[19]T. Hils, P. Böni, and J. Stahn, Physica B **350**, 166 (2004).

[20]N. Kardjilov, P. Böni, A. Hilger, M. Strobl, and W. Treimer, Nucl. Instrum. Methods Phys. Res. A **542**, 248 (2005).

[21]S. Mühlbauer, M. Stadlbauer, P. Böni, C. Schanzer, J. Stahn, and U. Filges, Physica B **385–386**, 1247 (2006).

[22]S. Mühlbauer, P. G. Niklowitz, M. Stadlbauer, R. Georgii, P. Link, J. Stahn, and P. Böni, Nucl. Instrum. Methods Phys. Res. A **586**, 77 (2008).

[23]K. Lefmann and K. Nielsen, Neutron News **10**, 20 (1999).

[24]A. Hilger, N. Kardjilov, M. Strobl, W. Treimer, and J. Banhart, Physica B **385–386**, 1213 (2006).

[25]http://www.swissneutronics.ch/fileadmin/download/snag_newsletter_2009–december.pdf